Engineering 6 (2020) 1013–1018

Contents lists available at ScienceDirect

Engineering

journal homepage: www.elsevier.com/locate/eng

Research
Energetic Materials and Interdisciplinary Science—Article

Metal-Free Hexagonal Perovskite High-Energetic Materials with $NH_3OH^+/NH_2NH_3^+$ as B-Site Cations

Yu Shang, Zhi-Hong Yu, Rui-Kang Huang, Shao-Li Chen *, De-Xuan Liu, Xiao-Xian Chen, Wei-Xiong Zhang *, Xiao-Ming Chen

MOE Key Laboratory of Bioinorganic and Synthetic Chemistry, School of Chemistry, Sun Yat-sen University, Guangzhou 510275, China

ARTICLE INFO

Article history:
Received 6 February 2020
Revised 25 April 2020
Accepted 27 May 2020
Available online 16 July 2020

Keywords:
Energetic materials
Single explosive
Solid propellant
Metal-free hexagonal perovskite

ABSTRACT

Designing and synthesizing more advanced high-energetic materials for practical use via a simple synthetic route are two of the most important issues for the development of energetic materials. Through an elaborate design and rationally selected molecular components, two new metal-free hexagonal perovskite compounds, which are named as DAP-6 and DAP-7 with a general formula of $(H_2dabco)B(ClO_4)_3$ (H_2dabco^{2+} = 1,4-diazabicyclo[2.2.2]octane-1,4-diium), were fabricated via an easily scaled-up synthetic route using NH_3OH^+ and $NH_2NH_3^+$ as B-site cations, respectively. Compared with their NH_4^+ analog ($(H_2dabco)(NH_4)(ClO_4)_3$; DAP-4), which has a cubic perovskite structure, DAP-6 and DAP-7 have higher crystal densities and enthalpies of formation, thus exhibiting higher calculated detonation performances. Specifically, DAP-7 has an ultrahigh thermal stability (decomposition temperatures (T_d) = 375.3 °C), a high detonation velocity (D = 8.883 km·s^{-1}), and a high detonation pressure (P = 35.8 GPa); therefore, it exhibits potential as a heat-resistant explosive. Similarly, DAP-6 has a high thermal stability (T_d = 245.9 °C) and excellent detonation performance (D = 9.123 km·s^{-1}, P = 38.1 GPa). Nevertheless, it also possesses a remarkably high detonation heat (Q = 6.35 kJ·g^{-1}) and specific impulse (I_{sp} = 265.3 s), which is superior to that of hexanitrohexaazaisowurtzitane (CL-20; Q = 6.23 kJ·g^{-1}, I_{sp} = 264.8 s). Thus, DAP-6 can serve as a promising high-performance energetic material for practical use.

1. Introduction

The development and production of energetic compounds with high energy density and stability are incredibly important because they play vital roles in both military and civil fields [1–3]. In the past few decades, research on energetic materials has experienced rapid progress, and the main achievements include high nitrogen-containing heterocycles [4–8], cage-strained molecules with more energetic groups (–NO_2, –NNO_2, –N_3, –$C(NO_2)_3$, etc.) [9], energetic salts [10–13], cocrystal explosives [14–19], and energetic coordination compounds [20–24]. However, the majority of energetic materials with excellent detonation performance tend to have low stability, complicated preparation methods, and high cost, which limit their practical application and make accessing advanced practicable high-energetic materials a great challenge.

Molecular perovskites with a general formula of ABX_3 provide a unique architectural platform, and their components can be customized to meet specific requirements, such as those for energetic materials. Molecular perovskites have been extensively studied due to their rich physical properties and potential applications [25–31]. Recently, we were the first to employ the perovskite structure to produce a dense packing of A-site fuel cations (i.e., H_2dabco^{2+} = 1,4-diazabicyclo[2.2.2]octane-1,4-diium) with triple X-site oxidative anions (i.e., ClO_4^-), which alternate at the molecular level. This condensed structure enabled fast and effective explosive reactions while maintaining high stability and low cost, as demonstrated by four molecular perovskite high-energetic materials, $(H_2dabco)M(ClO_4)_3$ (M = Na^+, K^+, Rb^+, and NH_4^+ for DAP-1, DAP-2, DAP-3, and DAP-4, respectively) [32–34]. In addition, we also briefly investigated the influence of A-site fuel cations on the oxygen balance (OB) with another two metal-containing perovskite compounds $(H_2pz)Na(ClO_4)_3$ (H_2pz^{2+} = piperazine-1,4-diium; PAP-1) and $(H_2dabco\text{-}O)K(ClO_4)_3$ ($H_2dabco\text{-}O^{2+}$ = 1-hydroxy-1,4-diazabicyclo[2.2.2]-octane-1,4-diium; DAP-O2) [35]. Among these

* Corresponding authors.
E-mail addresses: chenshli8@mail.sysu.edu.cn (S.-L. Chen), zhangwx6@mail.sysu.edu.cn (W.-X. Zhang).

https://doi.org/10.1016/j.eng.2020.05.018

six members, DAP-4, which is metal-free, shows particular promise in applications such as explosives and propellant components and thus has attracted considerable attention [36–38]. Nevertheless, the field of molecular perovskite high-energetic materials is still in its infancy and is thus replete with opportunities and challenges. As the detonation performance (typically the detonation pressure and the velocity) is positively correlated to the crystal density and formation enthalpy of energetic materials, increasing both of these parameters simultaneously in crystals is always one of the most important issues for designing advanced high-energetic materials [39,40]. Subsequently, to elucidate the relationship between the structural details and properties and obtain better overall performance than with DAP-4 [41], we designed and systematically investigated five metal-free compounds solely by changing the A-site organic cations in DAP-4, and found that improving the OB while keeping the spherical shape of A-site cations to match the anionic cages tends to yield a better overall detonation performance. However, it is difficult to increase the crystal density and formation enthalpy simultaneously, solely by adjusting the A-site cations; unfortunately, our previous results did not show a significant improvement in detonation performance.

The ABX_3-type perovskites have three typical subclasses featuring different linkages of the BX_6 octahedra [42]. In addition to the cubic structure (i.e., $CaTiO_3$ prototype) consisting of corner-sharing BX_6 octahedra, the hexagonal structure (i.e., $BaNiO_3$ prototype) consisting of face-sharing BX_6 octahedra is also a well-known and important model, and has the capacity to allow an alternate and dense packing of fuel and oxidative components at the molecular level. To explore new perovskite high-energetic compounds with a hexagonal structure, we focused on seeking derivatives of the NH_4^+ cation to serve as metal-free B-site cations. Compared with the NH_4^+ cation, the NH_3OH^+ and $NH_2NH_3^+$ cations have higher formation enthalpies and could form more hydrogen-bonding interactions in crystals; thus, they are favored for designing highly energetic materials [11,43,44]. With these cations, two new metal-free hexagonal perovskite high-energetic materials, $(H_2dabco)B(ClO_4)_3$ (B = NH_3OH^+ and $NH_2NH_3^+$ for DAP-6 and DAP-7, respectively, Fig. 1), were prepared with a one-step self-assembly process in aqueous solution under ambient conditions. To the best of our knowledge, DAP-6 and DAP-7 represent the first examples of perovskite compounds with NH_3OH^+ and $NH_2NH_3^+$, respectively, as B-site cations rather than A-site cations [45–49]. The structures, thermal stabilities, and energetic performances of DAP-6 and DAP-7 were studied experimentally and theoretically. DAP-6 and DAP-7 exhibit higher densities and formation enthalpies than the NH_4^+ analog ($(H_2dabco)(NH_4)(ClO_4)_3$; DAP-4) in the cubic structure and therefore possess higher detonation performances and excellent specific impulse (I_{sp}), which enable them to be promising candidates for practical explosives and propellants.

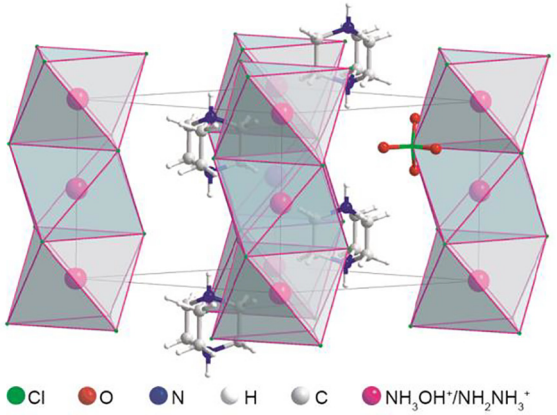

Fig. 1. The structure of metal-free hexagonal perovskite compounds (DAP-6 and DAP-7). For clarity, all X-site ClO_4^- anions except one are presented as small green spheres, while B-site cations (NH_3OH^+ and $NH_2NH_3^+$) are presented as magenta spheres.

2. Results and discussion

2.1. Single-crystal structures

The single crystals of DAP-6 and DAP-7 were obtained by the slow evaporation of the source solution after several days. The single-crystal X-ray crystallography at 223 K showed that DAP-6 and DAP-7 crystallize in the monoclinic space groups $P2_1$ and $P2_1/m$, respectively (Table 1) and that both possess a hexagonal perovskite-type structure (prototype phase $BaNiO_3$) with the formula ABX_3, with H_2dabco^{2+} as the A-site cation, NH_3OH^+ or $NH_2NH_3^+$ as the B-site cation, and ClO_4^- as the X-site anion. The crystal structures contain infinite linear $\{B(ClO_4)_3\}_n^{2n-}$ chains consisting of face-sharing $B(ClO_4)_6$ octahedra and H_2dabco^{2+} cations located in the interchain space (Fig. 1). As the effective radii of both NH_3OH^+ (216 pm) and $NH_2NH_3^+$ (217 pm) are much larger than that of NH_4^+ (146 pm) [50], both DAP-6 and DAP-7 adopt a hexagonal packing structure rather than the cubic one adopted by DAP-4, such that each $B(ClO_4)_6$ octahedron shares two faces with the adjacent octahedra to fulfill the hydrogen-bonding interactions in crystals (vide infra). The hydrogen-bonding interactions between NH_3OH^+ and ClO_4^- in DAP-6 seem to be stronger than those between $NH_2NH_3^+$ and ClO_4^- in DAP-7, as suggested by the fact that the shortest atomic distance d(N···O) is 2.88(5) Å (1 Å = 10^{-10} m) in DAP-6 and 3.020(5) Å in DAP-7 (Table 2). Accordingly, the linear $\{B(ClO_4)_3\}_n^{2n-}$ chains of DAP-6 can pack into the structure more compactly, resulting in a slightly higher crystal density (D_c) for DAP-6 (1.92 g·cm^{-3}) than for DAP-7 (1.90 g·cm^{-3})

Table 1
Crystallographic data and structural refinements for two metal-free hexagonal perovskite compounds.

Crystallographic/structural data	DAP-6	DAP-7
Formula	$C_6H_{18}Cl_3N_3O_{13}$	$C_6H_{19}Cl_3N_4O_{12}$
Formula weight (g·mol^{-1})	446.58	445.60
T (K)	223(2)	223(2)
λ (Å)	1.5418	1.5418
Crystal system	Monoclinic	Monoclinic
Space group	$P2_1$	$P2_1/m$
a (Å)	20.740(1)	10.378(2)
b (Å)	8.2366(2)	8.0505(7)
c (Å)	20.790(1)	10.587(2)
β (°)	119.65(1)	117.99(2)
V (Å^3)	3086.4(3)	781.0(2)
Z	8	2
D_c (g·cm^{-3})	1.922	1.895
Reflections collected	21 302	2 680
Independent reflection	11 111	1 604
R_{int}[a]	0.0490	0.0326
R_1 [$I > 2\sigma(I)$][a]	0.0765	0.0620
wR_2 [$I > 2\sigma(I)$][a]	0.1965	0.1694
R_1 (all data)[a]	0.0773	0.0638
wR_2 (all data)[a]	0.1975	0.1704
Goodness of fit	1.043	1.124
Completeness	1.00	0.99
CCDC	1 978 742	1 978 743

T: temperature; λ: wavelength; a, b, c: cell length; β: cell angle; V: cell volume; Z: formula units; D_c: crystal density; R_{int}: merging residual value; R_1: unweighted residual factor; wR_2: weighted residual factor; I: intensity of reflection; $\sigma(I)$: estimated standard uncertainty of the reflection; CCDC: Cambridge Crystallographic Data Centre.

[a] $R_{int} = \Sigma|F_o^2 - \langle F_o^2\rangle|/\Sigma F_o^2$; $R_1 = \Sigma||F_o| - |F_c||/\Sigma|F_o|$; $wR_2 = \{\Sigma w[(F_o)^2 - (F_c)^2]^2/\Sigma w[(F_o)^2]^2\}^{1/2}$; where F_o and F_c are the experimental and calculated structural factors, respectively, and w is a weight factor.

Table 2
Selected hydrogen-bond geometries for the B-site cations in DAP-6 and DAP-7 at 223 K.

D–H···A[a]	d(D···A) (Å)	∠D–H···A (°)
DAP-6		
N3–H3D···O23	2.93(2)	129.2
N3–H3C···O37a	3.06(2)	127.0
N3–H3E···O31a	3.07(2)	153.8
N6–H6C···O19b	2.96(2)	154.5
N6–H6E···O36a	2.96(2)	160.0
N6–H6D···O3c	2.97(2)	123.2
N9–H9E···O47d	2.88(5)	139.5
N9–H9C···O52d	2.98(3)	126.7
N9–H9C···O13	2.98(6)	130.4
N12–H12E···O10	2.91(2)	128.7
N12–H12C···O25	2.98(2)	129.2
N12–H12D···O27e	3.05(3)	159.1
O49–H49···O32	3.00(2)	132.2
O49–H49···O37a	3.01(2)	129.0
O50–H50···O20	3.14(2)	133.7
O51–H51···O26	3.05(2)	147.5
O52–H52···O45	2.94(3)	135.8
DAP-7		
N1–H1C···N1f	3.14(1)	153.9
N1–H1D···O9g	3.086(6)	158.1
N1–H1E···O3	3.020(5)	132.8

Symmetry codes: a: 1 − *x*, *y* + 1/2, 1 − *z*; b: −*x*, *y* + 1/2, −*z*; c: 1 − *x*, *y* + 1/2, −*z*; d: 1 − *x*, *y* − 1/2, −*z*; e: 2 − *x*, *y* + 1/2, 1 − *z*; f: *x*, 1/2 − *y*, *z*; g: 1 − *x*, −*y*, 1 − *z*.

[a] D, H, and A stands for donor atom, hydrogen atom, and acceptor atom related in the hydrogen-bonding interactions.

calculated by single-crystal X-ray crystallography at 223 K. This fact was further confirmed by the density for DAP-6 (1.90 g·cm^{-3}) and DAP-7 (1.87 g·cm^{-3}) from Pawley refinements on capillary powder X-ray diffraction data collected at 298 K (Table S1 in Appendix A).

Few studies have investigated the non-quasi-spherical units that rarely act as B-site cations in perovskites. To further understand the weak interactions around B-site cations, Hirshfeld surface analyses were performed for the NH_3OH^+ cations in DAP-6 and the $NH_2NH_3^+$ cations in DAP-7. The surfaces are mapped with normalized contact distance, d_{norm} (Fig. 2), in a red-white-blue scheme indicating the intermolecular contacts shorter (red), around (white), and longer (blue) than the van der Waals separation. The asymmetric unit of DAP-6 or DAP-7 includes four NH_3OH^+ or one half $NH_2NH_3^+$ cations, respectively. As suggested by the numerous large red spots on Hirshfeld surfaces (Fig. 2), in both DAP-6 and DAP-7, very high percentages (average value of 82.4% for four NH_3OH^+ cations and 89.5% for one $NH_2NH_3^+$ cation, respectively) of the surface area were found associating with H···O/N and O/N···H short-contacts, which denote electrostatically attractive hydrogen-bonding interactions between the B-site cations and the adjacent ClO_4^- anions and/or B-site cations. Similarly, Hirshfeld surface analyses for the A-site cations (H_2dabco^{2+}) in DAP-6 and DAP-7 indicated that each A-site cation also forms abundant hydrogen-bonding interactions with adjacent perchlorate anions, as suggested by the attractive H···O contacts associating with 86.1% and 82.2% of the surface area for DAP-6 and DAP-7, respectively. In short, together with the attractive Coulomb interactions between cations and anions, these abundant hydrogen-bonding interactions facilitate the close packing of the face-sharing $B(ClO_4)_6$ octahedra along the infinite linear $\{B(ClO_4)_3\}_n^{2n-}$ chains, which are further closely packed with the interchain H_2dabco^{2+} cations and result in high crystal densities for both DAP-6 and DAP-7.

2.2. Thermal stability and long-term stability

The thermal behaviors of DAP-6 and DAP-7 were characterized by differential thermal analysis (DTA) with a heating rate of 5 °C·min^{-1}. As shown in Table 3 [3,10,32,41], the onset decomposition temperatures (T_d) of DAP-6 and DAP-7 are 245.9 and 375.3 °C, respectively, which are higher than those of cyclotrimethylene trinitramine (RDX; 210.0 °C) and hexanitrohexaazaisowurtzitane (CL-20; 215.0 °C), [10] due to their strong intra-ionic covalent bonds, the inter-ionic attractive Coulombic interactions, and the aforementioned abundant

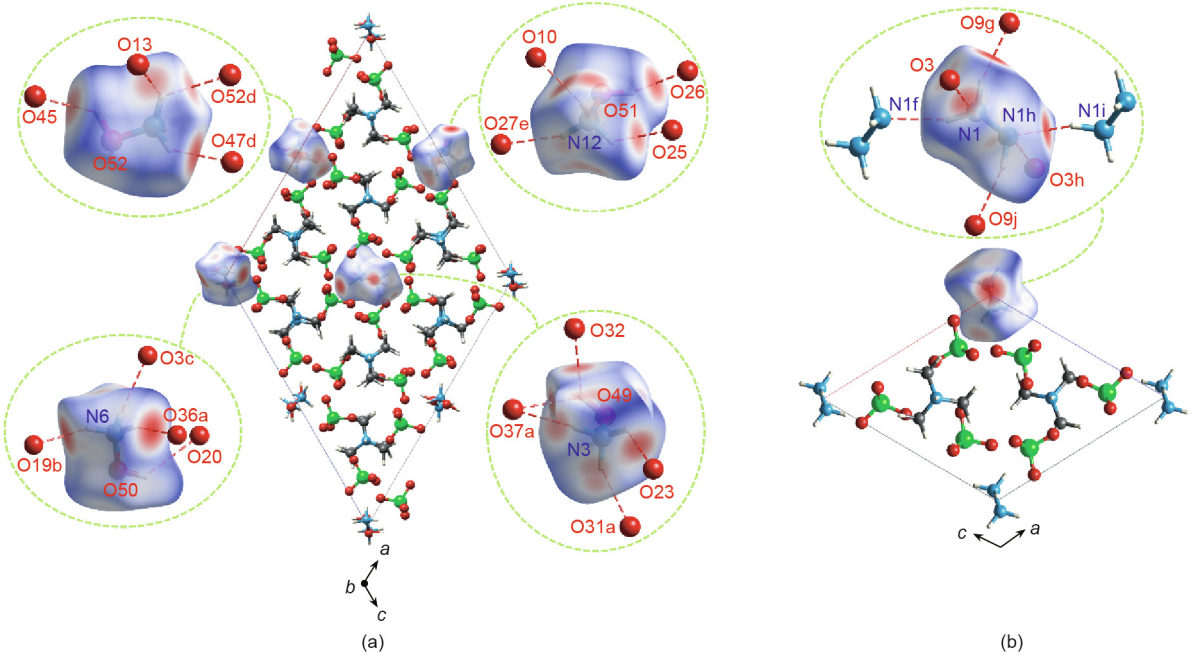

Fig. 2. The Hirshfeld surfaces mapped with d_{norm} for (a) NH_3OH^+ cations in DAP-6 and (b) $NH_2NH_3^+$ cations in DAP-7, where the red and blue spots represent the intermolecular contacts shorter and longer than van der Waals separations, respectively. Symmetry codes: a: 1 − *x*, *y* + 1/2, 1 − *z*; b: −*x*, *y* + 1/2, −*z*; c: 1 − *x*, *y* + 1/2, −*z*; d: 1 − *x*, *y* − 1/2, −*z*; e: 2 − *x*, *y* + 1/2, 1 − *z*; f: *x*, 1/2 − *y*, *z*; g: 1 − *x*, −*y*, 1 − *z*; h: −*x*, −*y*, −*z*; i: −*x*, −1/2 + *y*, −*z*; j: *x* − 1, +*y*, −1 + *z*.

Table 3
Detonation properties of three classic organic explosives, DAP-4, DAP-O4, DAP-6, and DAP-7.

Compound	ρ (g·cm^{-3})	T_d (°C)	Q (kJ·g^{-1})	D (km·s^{-1})	P (GPa)	I_{sp} (s)	OB (%)[c]	IS (J)	FS (N)
RDX	1.82 [3]	210.0 [10]	5.59	8.634	33.3	251.1	−21.6	7.5 [10]	120 [10]
HMX	1.90 [3]	279.0 [10]	5.57	8.892	36.2	250.8	−21.6	7.0 [10]	112 [10]
CL-20	2.04 [3]	215.0 [10]	6.23	9.507	43.1	264.8	−11.0	4.0 [10]	48 [10]
DAP-4	1.87[a]	358.4[b]	5.87	8.806	35.2	253.6	−27.9	23.0 [32,41]	36 [32,41]
DAP-O4	1.85[a]	351.6[b]	6.21	8.900	35.7	262.5	−23.3	17.5 [32,41]	≤ 5 [32,41]
DAP-6	1.90[a]	245.9[b]	6.35	9.123	38.1	265.3	−23.3	12.0	≤ 5
DAP-7	1.87[a]	375.3[b]	6.00	8.883	35.8	256.9	−28.7	27.5	≤ 5

ρ: crystal density; Q: detonation heat; D: detonation velocity; P: detonation pressure; IS: impact sensitivity; FS: friction sensitivity; HMX: cyclotetramethylene tetranitramine; DAP-O4: $(H_2dabco\text{-}O)(NH_4)(ClO_4)_3$ ($H_2dabco\text{-}O^{2+}$ = 1-hydroxy-1,4-diazabicyclo[2.2.2]-octane-1,4-diium).
[a] The crystal densities estimated from capillary powder X-ray diffraction (PXRD) data collected at room temperature.
[b] The onset decomposition temperatures evaluated from DTA (5 °C·min^{-1}).
[c] Oxygen balance based on CO_2 for $C_aH_bN_cCl_dO_e$: OB = 1600[$e - 2a - (b - d)/2$]/M_W, where M_W is molecular weight.

hydrogen-bonding interactions. In addition, the powder samples of DAP-6 and DAP-7 had been stored at ambient conditions for three and five months, respectively, and their powder X-ray diffraction (PXRD) patterns are almost the same as those of the as-synthesized samples (Figs. S1 and S2 in Appendix A), suggesting long-term stabilities under ambient conditions for both DAP-6 and DAP-7.

2.3. Detonation parameters

The detonation parameters of DAP-6 and DAP-7 were calculated using the density function theory (DFT) and the extended Kamlet–Jacobs (K–J) equation, and the results are shown in Table 3. The results suggested that DAP-7 has higher detonation heat, detonation velocity, and detonation pressure than that of RDX, while DAP-6 has a better detonation performance than that of cyclotetramethylene tetranitramine (HMX). In particular, DAP-6 possesses a remarkably high detonation heat (6.35 kJ·g^{-1}), which is superior to that of all previously reported perovskite energetic materials and even that of CL-20 (6.23 kJ·g^{-1}).

To further reveal the effects of the molecular components on the detonation performance for DAP-6 and DAP-7, a previously reported compound, $(H_2dabco\text{-}O)(NH_4)(ClO_4)_3$ ($H_2dabco\text{-}O^{2+}$ = 1-hydroxy-1,4-diazabicyclo[2.2.2]-octane-1,4-diium; DAP-O4), which has the highest detonation performance among the six previously known metal-free perovskite energetic compounds [32,41], was compared with DAP-6 and DAP-7. As shown in Fig. 3, in view of the molecular components, DAP-6 could be regarded as a modified version of DAP-O4 by moving the oxygen atom from the A-site $H_2dabco\text{-}O^{2+}$ cation to the B-site NH_4^+ cation; thus, DAP-6 and DAP-O4 are isomers with a same empirical chemical formula and the same OB (−23.3%). However, all detonation parameters of DAP-6 are higher than those of DAP-O4, presenting a new record for perovskite energetic compounds. Such an improvement on the detonation performances from DAP-O4 to DAP-6 mainly comes from the increase of both formation enthalpy and crystal density. Specifically, the formation enthalpies of both NH_3OH^+ (669.5 kJ·mol^{-1}) and H_2dabco^{2+} (1657.5 kJ·mol^{-1}) cations in DAP-6 are higher than those of the corresponding NH_4^+ (626.4 kJ·mol^{-1}) and $H_2dabco\text{-}O^{2+}$ (1626.3 kJ·mol^{-1}) cations in DAP-O4 (see Table S2 and Fig. S3 in Appendix A). Additionally, DAP-6 has a higher crystal density (1.90 g·cm^{-3}) than that of DAP-O4 (1.85 g·cm^{-3}), likely due to its hexagonal dense packing model, which further contributes to its improved detonation performance. Similarly, compared with DAP-4, although DAP-7 has the similar crystal density (1.87 g·cm^{-3}) and even a slightly lower OB (−27.9% for DAP-4 vs −28.7% for DAP-7), the detonation parameters of DAP-7 are slightly higher than those of DAP-4, because of the higher formation enthalpy of the $NH_2NH_3^+$ cation (770.0 kJ·mol^{-1}) in DAP-7 than that of the NH_4^+ cation in DAP-4 (see Table S2).

2.4. Specific impulse

The I_{sp}, an important parameter indicating the performance of solid propellants, was calculated for each material using EXPLO5^{TM} v6.04.02 code based on the heat of formation back-calculated from the assumed detonation reactions (see Tables S3–S5 in Appendix A). As shown in Table 3, DAP-7 has a calculated specific impulse (256.9 s) higher than that of DAP-4 (253.6 s) and HMX (250.8 s), while DAP-6 has an even higher calculated specific impulse of 265.3 s, which is not only higher than that of its isomer, DAP-O4 (262.5 s), but is even comparable to that of CL-20 (264.8 s). Such high performances of the new solid propellants, DAP-6 and DAP-7, could be ascribed to their high decomposition heats, which benefit from the aforementioned high formation enthalpies of the cations. Notably, DAP-6 and DAP-7 have much higher hydrogen contents (4.03% and 4.26%, respectively) than that of CL-20 (1.4%). They, therefore, can yield more water vapor among the

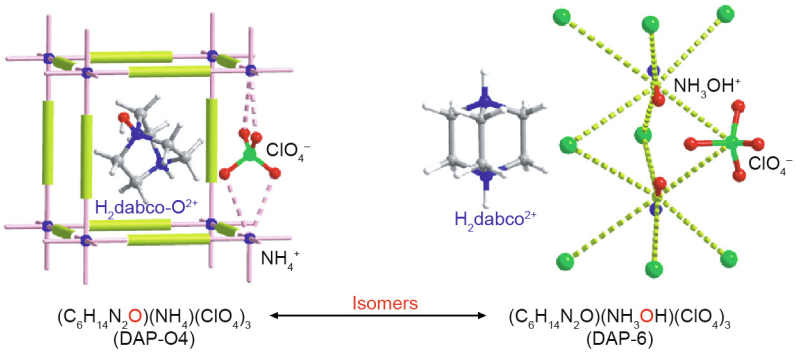

Fig. 3. Isomeric relationship between DAP-6 in the hexagonal perovskite structure and DAP-O4 in the cubic perovskite structure.

combustion products, which then have a lower average molecular weight, making an additional contribution to their high specific impulses.

2.5. Sensitivities

The impact and friction sensitivities were tested on a BFH-10 BAM impact tester (OZM Research S.R.O., Czech Republic) and an FSKM-10 BAM friction apparatus (OZM Research S.R.O., Czech Republic), respectively. As listed in Table 3, the impact sensitivities of DAP-6 and DAP-7 were 12.0 and 27.5 J, respectively, suggesting they are more insensitive to impact than the typical high explosives such as RDX (7.5 J), HMX (7.0 J), and CL-20 (4.0 J). In contrast, similar to other molecular perovskite energetic materials, DAP-6 and DAP-7 seem to be sensitive to friction ($FS \leq 5$ N), which is probably associated with the relatively rigid perovskite structure and its perchlorate component.

3. Conclusions

In summary, by elaborately designing and choosing the molecular components, two new metal-free hexagonal perovskite high-energetic materials, namely DAP-6 and DAP-7, were successfully fabricated for the first time using NH_3OH^+ and $NH_2NH_3^+$ cations, respectively, as the B-site cations. The calculated detonation performances of DAP-6 and DAP-7 are better than that of the NH_4^+ analog (DAP-4), which has a cubic perovskite structure, due to their molecular assembly in denser hexagonally close-packed structures and cations with higher formation enthalpies. Because of the good thermal stability (T_d = 245.9 and 375.3 °C) and detonation performance (D = 9.123 and 8.883 km·s^{-1}, P = 38.1 and 35.8 GPa), DAP-6 and DAP-7 are promising candidates for practical usage as explosives and propellants. In particular, DAP-6 has higher crystal density and formation enthalpy than isomeric DAP-O4, which has a cubic perovskite structure, and it exhibits a new record of detonation performance metrics among perovskite energetic compounds, particularly a remarkably high detonation heat (Q = 6.35 kJ·g^{-1}) and a specific impulse (I_{sp} = 265.3 s) superior to that of CL-20 (Q = 6.23 kJ·g^{-1}, I_{sp} = 264.8 s). The dense molecular arrangements of DAP-6 and DAP-7, together with the resulting high detonation parameters and specific impulses, show that the hexagonal perovskite structure may serve as a new promising model to tune the crystal density, OB, formation enthalpy, and eventually, the energetic performance for the development of advanced high-energetic materials in the future.

Acknowledgements

This work was supported by the National Natural Science Foundation of China (21722107 and 21821003), the Local Innovative and Research Teams Project of Guangdong Pearl River Talents Program (2017BT01C161), and the Natural Science Foundation of Guangdong Province of China (2020A1515010460).

Compliance with ethics guidelines

Yu Shang, Zhi-Hong Yu, Rui-Kang Huang, Shao-Li Chen, De-Xuan Liu, Xiao-Xian Chen, Wei-Xiong Zhang, and Xiao-Ming Chen declare that they have no conflict of interest or financial conflicts to disclose.

Appendix A. Supplementary data

Supplementary data to this article can be found online at https://doi.org/10.1016/j.eng.2020.05.018.

References

[1] Klapötke TM. High energy density materials. Berlin: Springer; 2007.
[2] Agrawal JP. High energy materials: propellants, explosives and pyrotechnics. New York: John Wiley & Sons; 2010.
[3] Meyer R, Köhler J, Homburg A. Explosives. New York: John Wiley & Sons; 2016.
[4] Zhang W, Zhang J, Deng M, Qi X, Nie F, Zhang Q. A promising high-energy-density material. Nat Commun 2017;8(1):181.
[5] Wang Y, Liu Y, Song S, Yang Z, Qi X, Wang K, et al. Accelerating the discovery of insensitive high-energy-density materials by a materials genome approach. Nat Commun 2018;9(1):2444.
[6] Tang Y, Kumar D, Shreeve JM. Balancing excellent performance and high thermal stability in a dinitropyrazole fused 1,2,3,4-tetrazine. J Am Chem Soc 2017;139(39):13684–7.
[7] Tang Y, He C, Imler GH, Parrish DA, Shreeve JM. A C–C bonded 5,6-fused bicyclic energetic molecule: exploring an advanced energetic compound with improved performance. Chem Commun 2018;54(75):10566–9.
[8] He C, Yin P, Mitchell LA, Parrish DA, Shreeve JM. Energetic aminated-azole assemblies from intramolecular and intermolecular N–HO and N–HN hydrogen bonds. Chem Commun 2016;52(52):8123–6.
[9] Yang J, Gong X, Mei H, Li T, Zhang J, Gozin M. Design of zero oxygen balance energetic materials on the basis of Diels–Alder chemistry. J Org Chem 2018;83(23):14698–702.
[10] Fischer N, Fischer D, Klapötke TM, Piercey DG, Stierstorfer J. Pushing the limits of energetic materials—the synthesis and characterization of dihydroxylammonium 5,5′-bistetrazole-1,1′-diolate. J Mater Chem 2012;22(38):20418.
[11] Yang C, Zhang C, Zheng Z, Jiang C, Luo J, Du Y, et al. Synthesis and characterization of cyclo-pentazolate salts of NH_4^+, NH_3OH^+, $N_2H_5^+$, $C(NH_2)_3^+$, and $N(CH_3)_4^+$. J Am Chem Soc 2018;140(48):16488–94.
[12] Wang Q, Shao Y, Lu M. Amino-tetrazole functionalized fused triazolo-triazine and tetrazolo–triazine energetic materials. Chem Commun 2019;55(43):6062–5.
[13] Xu Y, Wang P, Lin Q, Du Y, Lu M. Cationic and anionic energetic materials based on a new amphotère. Sci China Mater 2019;62(5):751–8.
[14] Bennion JC, Siddiqi ZR, Matzger AJ. A melt castable energetic cocrystal. Chem Commun 2017;53(45):6065–8.
[15] Landenberger KB, Bolton O, Matzger AJ. Energetic–energetic cocrystals of diacetone diperoxide (DADP): dramatic and divergent sensitivity modifications via cocrystallization. J Am Chem Soc 2015;137(15):5074–9.
[16] Bolton O, Matzger AJ. Improved stability and smart-material functionality realized in an energetic cocrystal. Angew Chem Int Ed Engl 2011;50(38):8960–3.
[17] Bellas MK, Matzger AJ. Achieving balanced energetics through cocrystallization. Angew Chem Int Ed Engl 2019;58(48):17185–8.
[18] Ma P, Jiang JC, Zhu SG, Zhu SG. Synthesis, XRD and DFT studies of a novel cocrystal energetic perchlorate amine salt: methylamine triethylenediamine triperchlorate. Combust Explos Shock Waves 2017;53(3):319–28.
[19] Ma P, Zhang L, Zhu S, Chen H. Synthesis, crystal structure and DFT calculation of an energetic perchlorate amine salt. J Cryst Growth 2011;335(1):70–4.
[20] Bushuyev OS, Brown P, Maiti A, Gee RH, Peterson GR, Weeks BL, et al. Ionic polymers as a new structural motif for high-energy-density materials. J Am Chem Soc 2012;134(3):1422–5.
[21] Li S, Wang Y, Qi C, Zhao X, Zhang J, Zhang S, et al. 3D energetic metal–organic frameworks: synthesis and properties of high energy materials. Angew Chem Int Ed Engl 2013;52(52):14031–5.
[22] Zhang J, Du Y, Dong K, Su H, Zhang S, Li S, et al. Taming dinitramide anions within an energetic metal–organic framework: a new strategy for synthesis and tunable properties of high energy materials. Chem Mater 2016;28(5):1472–80.
[23] Xu JG, Sun C, Zhang MJ, Liu BW, Li XZ, Lu J, et al. Coordination polymerization of metal azides and powerful nitrogen-rich ligand toward primary explosives with excellent energetic performances. Chem Mater 2017;29(22):9725–33.
[24] Xu Y, Wang Q, Shen C, Lin Q, Wang P, Lu M. A series of energetic metal pentazolate hydrates. Nature 2017;549(7670):78–81.
[25] Lee MM, Teuscher J, Miyasaka T, Murakami TN, Snaith HJ. Efficient hybrid solar cells based on meso-superstructured organometal halide perovskites. Science 2012;338(6107):643–7.
[26] Wu Y, Shaker S, Brivio F, Murugavel R, Bristowe PD, Cheetham AK. $[Am]Mn(H_2PO_2)_3$: a new family of hybrid perovskites based on the hypophosphite ligand. J Am Chem Soc 2017;139(47):16999–7002.
[27] Ye HY, Tang YY, Li PF, Liao WQ, Gao JX, Hua XN, et al. Metal-free three-dimensional perovskite ferroelectrics. Science 2018;361(6398):151–5.
[28] Du ZY, Zhao YP, Zhang WX, Zhou HL, He CT, Xue W, et al. Above-room-temperature ferroelastic phase transition in a perovskite-like compound $[N(CH_3)_4][Cd(N_3)_3]$. Chem Commun 2014;50(16):1989–91.

[29] Xu WJ, Li PF, Tang YY, Zhang WX, Xiong RG, Chen XM, et al. A molecular perovskite with switchable coordination bonds for high-temperature multiaxial ferroelectrics. J Am Chem Soc 2017;139(18):6369–75.
[30] Szafrański M. Synthesis, crystal structures, and phase transitions of dabco oxonium triperchlorate and tritetrafluoroborate. Cryst Growth Des 2018;18 (11):7106–13.
[31] Yang WS, Park BW, Jung EH, Jeon NJ, Kim YC, Lee DU, et al. Iodide management in formamidinium-lead-halide-based perovskite layers for efficient solar cells. Science 2017;356(6345):1376–9.
[32] Chen SL, Yang ZR, Wang BJ, Shang Y, Sun LY, He CT, et al. Molecular perovskite high-energetic materials. Sci China Mater 2018;61(8):1123–8.
[33] Zhang WX, Chen SL, Chen XM, inventors; Wanhuida Law Firm, assignee. Use of type of compounds as energetic material. China patent CN201610665880.3. 2016 Aug 12. Chinese.
[34] Chen SL, Zhang WX, Chen XM. Exceptional thermal energy storage in a series of perovskite-type perchlorate cage compounds: $[H_{14}C_6N_2][M(ClO_4)_3]$ (M = Na/K/Rb). In: Proceedings of the 9th National Conference in Inorganic Chemistry—B Coordination Chemistry; 2015 Jul 25–29; Nanchang, China. Beijing: Chinese Chemical Society; 2015. Chinese.
[35] Chen SL, Shang Y, He CT, Sun LY, Ye ZM, Zhang WX, et al. Optimizing the oxygen balance by changing the A-site cations in molecular perovskite high-energetic materials. Cryst Eng Comm 2018;20(46):7458–63.
[36] Li X, Hu S, Cao X, Hu L, Deng P, Xie Z. Ammonium perchlorate-based molecular perovskite energetic materials: preparation, characterization, and thermal catalysis performance with MoS_2. J Energ Mater 2020;38(2):162–9.
[37] Deng P, Ren H, Jiao Q. Enhanced the combustion performances of ammonium perchlorate-based energetic molecular perovskite using functionalized graphene. Vacuum 2019;169:108882.
[38] Zhou J, Ding L, Zhao F, Wang B, Zhang J. Thermal studies of novel molecular perovskite energetic material $(C_6H_{14}N_2)[NH_4(ClO_4)_3]$. Chin Chem Lett 2019;31 (2):554–8.
[39] Fershtat LL, Makhova NN. 1,2,5-Oxadiazole-based high-energy-density materials: synthesis and performance. ChemPlusChem 2020;85(1):13–42.
[40] Xu J, Zheng S, Huang S, Tian Y, Liu Y, Zhang H, et al. Host-guest energetic materials constructed by incorporating oxidizing gas molecules into an organic lattice cavity toward achieving highly-energetic and low-sensitivity performance. Chem Commun 2019;55(7):909–12.
[41] Shang Y, Huang RK, Chen SL, He CT, Yu ZH, Ye ZM, et al. Metal-free molecular perovskite high-energetic materials. Cryst Growth Des 2020;20(3):1891–7.
[42] Wang SS, Chen XX, Huang B, Huang RK, Zhang WX, Chen XM. Unique freezing dynamics of flexible guest cations in the first molecular postperovskite ferroelectric: $(C_5H_{13}NBr)[Mn(N(CN)_2)_3]$. CCS Chem 2019;1(4):448–54.
[43] Zhang J, Mitchell LA, Parrish DA, Shreeve JM. Enforced layer-by-layer stacking of energetic salts towards high-performance insensitive energetic materials. J Am Chem Soc 2015;137(33):10532–5.
[44] Zhang J, Zhang Q, Vo TT, Parrish DA, Shreeve JM. Energetic salts with π-stacking and hydrogen-bonding interactions lead the way to future energetic materials. J Am Chem Soc 2015;137(4):1697–704.
[45] Svane KL, Forse AC, Grey CP, Kieslich G, Cheetham AK, Walsh A, et al. How strong is the hydrogen bond in hybrid perovskites? J Phys Chem Lett 2017;8 (24):6154–9.
[46] Kieslich G, Forse AC, Sun S, Butler KT, Kumagai S, Wu Y, et al. Role of amine-cavity interactions in determining the structure and mechanical properties of the ferroelectric hybrid perovskite $[NH_3NH_2]Zn(HCOO)_3$. Chem Mater 2016;28 (1):312–7.
[47] Liu B, Shang R, Hu KL, Wang ZM, Gao S. A new series of chiral metal formate frameworks of $[HONH_3][M(II)(HCOO)_3]$ (M = Mn, Co, Ni, Zn, and Mg): synthesis, structures, and properties. Inorg Chem 2012;51(24):13363–72.
[48] Trzmiel J, Sieradzki A, Pawlus S, Mączka M. Insight into understanding structural relaxation dynamics of $[NH_2NH_3][Mn(HCOO)_3]$ metal–organic formate. Mater Sci Eng B 2018;236–237:24–31.
[49] Tenuta E, Zheng C, Rubel O. Thermodynamic origin of instability in hybrid halide perovskites. Sci Rep 2016;6(1):37654.
[50] Kieslich G, Sun S, Cheetham AK. Solid-state principles applied to organic–inorganic perovskites: new tricks for an old dog. Chem Sci 2014;5 (12):4712–5.